**iScience, Volume *23***

## Supplemental Information

# Obesity Reshapes Visceral Fat-Derived MHC I Associated-Immunopeptidomes and Generates Antigenic Peptides to Drive $CD8^+$ T Cell Responses

**Xiaoling Chen, Shufeng Wang, Yi Huang, Xia Zhao, Xu Jia, Gang Meng, Qian Zheng, Mengjun Zhang, Yuzhang Wu, and Li Wang**

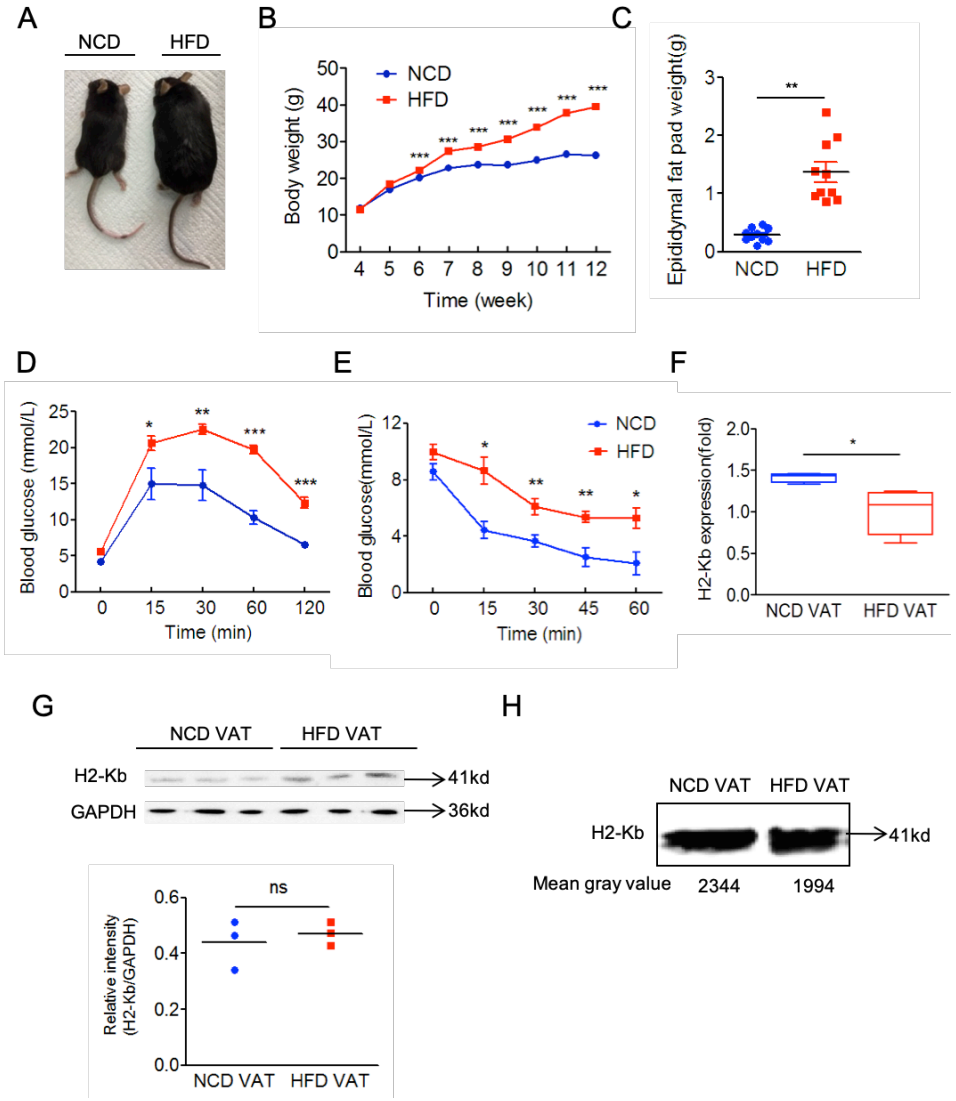


**Figure S1. Establishment of high fat diet (HFD)-induced obese C57BL/6 mice model, Related to Figure 1**

(A) Representative images of C57BL/6 male mice fed with a high-fat diet (HFD) or a normal diet (NCD) beginning at 4 weeks of age for 8 weeks. (B) Body weight gain of male C57BL/6 mice after 8-week HFD or NCD feeding (started at 4 weeks of age) (n=10 mice per group). The epididymal fat pad (VAT) mass from male C57BL/6 mice with HFD or NCD feeding at 12 weeks of age. (n=10 mice per group). Serum glucose levels during (D) glucose tolerance test (GTT) and (E) insulin tolerance test (ITT) in male C57BL/6 mice after 8-week HFD (n=10 mice per group). Data are means and error bars are ±SEM. Quantitative real-time PCR analysis (n=10 mice per group) (F) and immunoblotting analyses (n=3 mice per group) (G) of H2-Kb expression in the VAT of mice after 8-week HFD or NCD feeding. (H) Immunoblotting analyses of H2-Kb in Co-IP ultrafiltration superfluid from the VAT homogenates of mice after 8-week HFD or NCD feeding.

* $p < 0.05$, ** $p < 0.01$, *** $p<0.0001$, and ns: no significance, determined by Student's t-test.

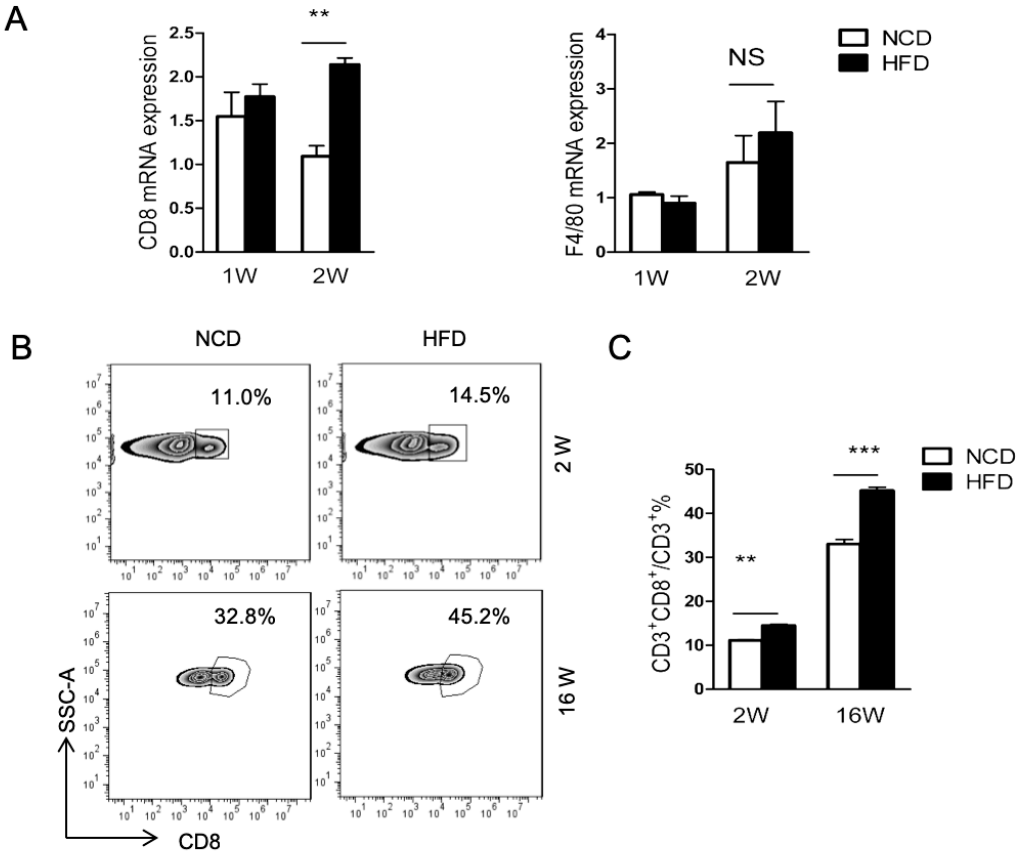


**Figure S2. HFD feeding induces an early increase of $CD8^+$ T cells in visceral adipose tissues, Related to Figure 3**

(A) Quantitative real-time PCR analysis of CD8 and F4/80 expression in the epididymal fat pads from mice fed with NCD and HFD for 1 or 2 weeks (started at 4 weeks of age) (n=10 mice per group). Data are means and error bars are ±SEM. Student's t test, *p < 0.05 and **p < 0.01, ***P<0.0001

(B) Representative FACS analysis of the proportion of infiltrated CD8+ T cells in the epididymal fat pads from mice fed with NCD and HFD for 2 or 16 weeks (started at 4 weeks of age). (C) Summary graph for FACS analysis of the frequency of infiltrated CD8+ T cells in the epididymal fat pads from mice fed with NCD and HFD for 2 and 16 weeks. Data are means and error bars are ±SEM.

* p < 0.05, ** p < 0.01, *** p<0.0001, and NS: no significance, determined by Student's t-test.

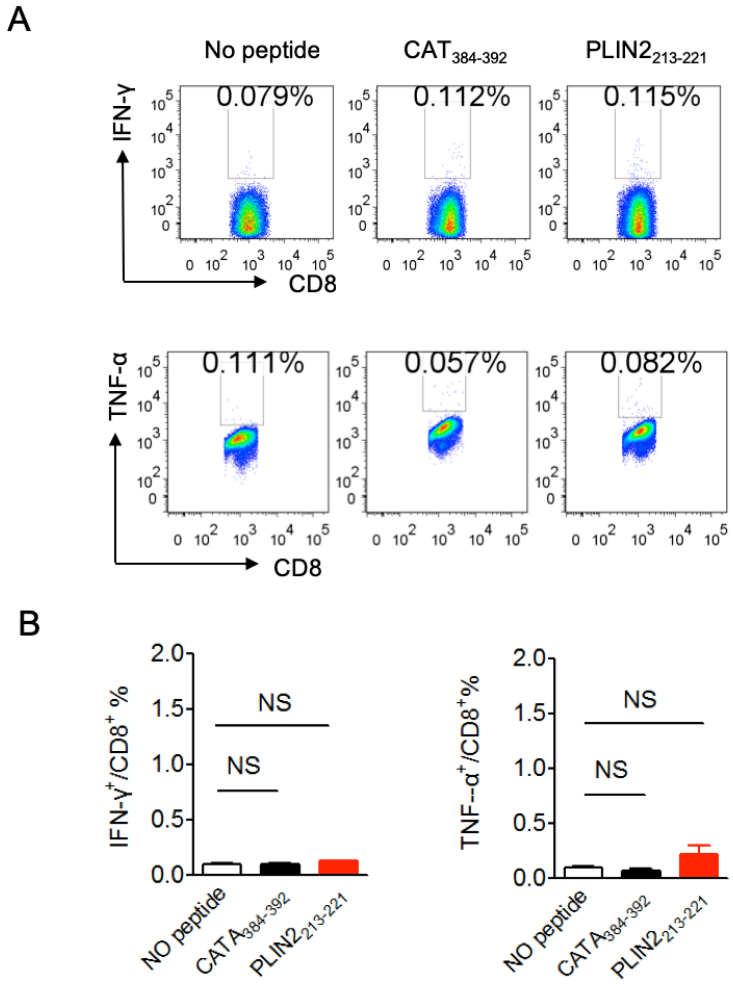


**Figure S3. The peptides shared by VAT-MIPs from both NCD and HFD-fed mice have no ability to prime CD8$^+$ T cells response, Related to Figure 4**

(A) Representative FACS plots indicating intracellular IFN-γ and TNF-α staining of CD8$^+$ T cells stimulated with the indicated peptides-loaded RAMS cells.

(B) Summary graph for FACS analysis of the frequency of IFN-γ and TNF-α-producing cells among CD8$^+$ T cells stimulated with the indicated peptides. Each bar represents the mean ± SEM of three independent experiments. NS: no significance, determined by Student's t-test.

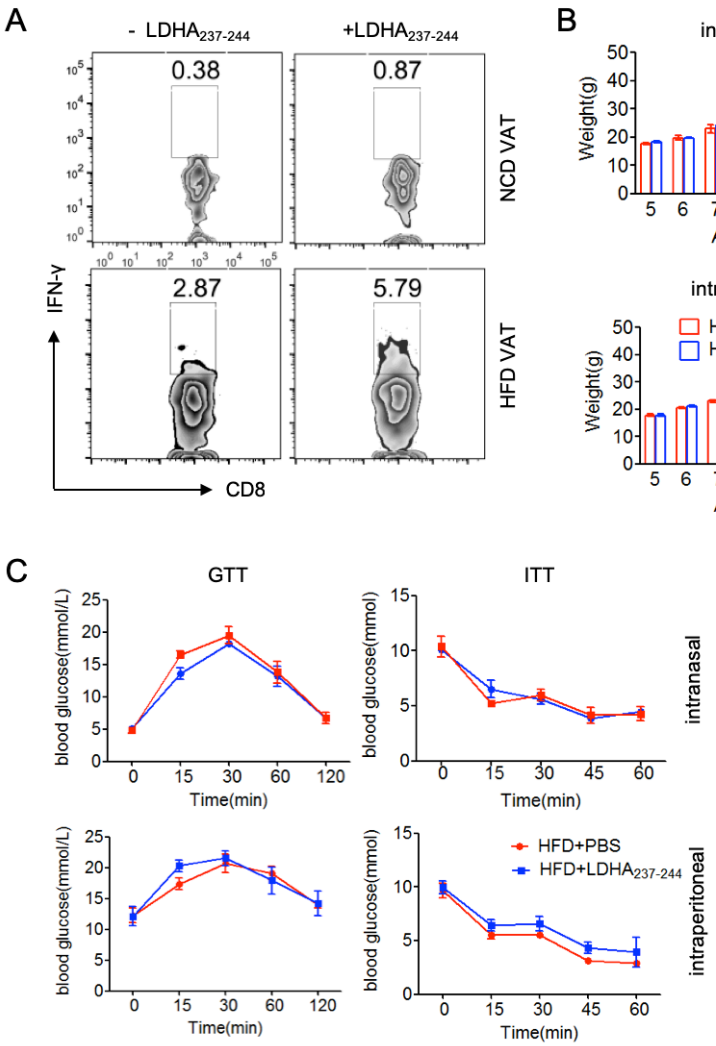


**Figure S4. Intranasal or intraperitoneal administration of a single $LDHA_{237-244}$ peptide fails to affect the weight gain, glucose intolerance and insulin resistance in HFD-fed obese mice, Related to Figure 5**

(A) Representative FACS indicating intracellular IFN-γ staining of VAT-infiltrated $CD8^+$ T cells stimulated with RMAS cells with RMAS cells loaded with or without $LDHA_{237-244}$ peptide.

(B) Comparison of changes in body weight between high-fat diet (HFD)-fed mice treated intranasally (upper) or intraperitoneally (lower) with $LDHA_{237-244}$ and PBS (n=4-5 mice per group). Error bars represent means ± SEM.

(C) Results of glucose tolerance (GTT) (i.p. 1 g per kg glucose, after 16 h fasting) and insulin tolerance (ITT) (i.p.,0.75 U insulin per kg body weight, after 3.5 h fasting) tests in HFD-fed mice treated intranasally (upper) or intraperitoneally (lower) with $LDHA_{237-244}$ and PBS (n =5 mice per group). Error bars represent means ± SEM. Data are representative of two experiments.

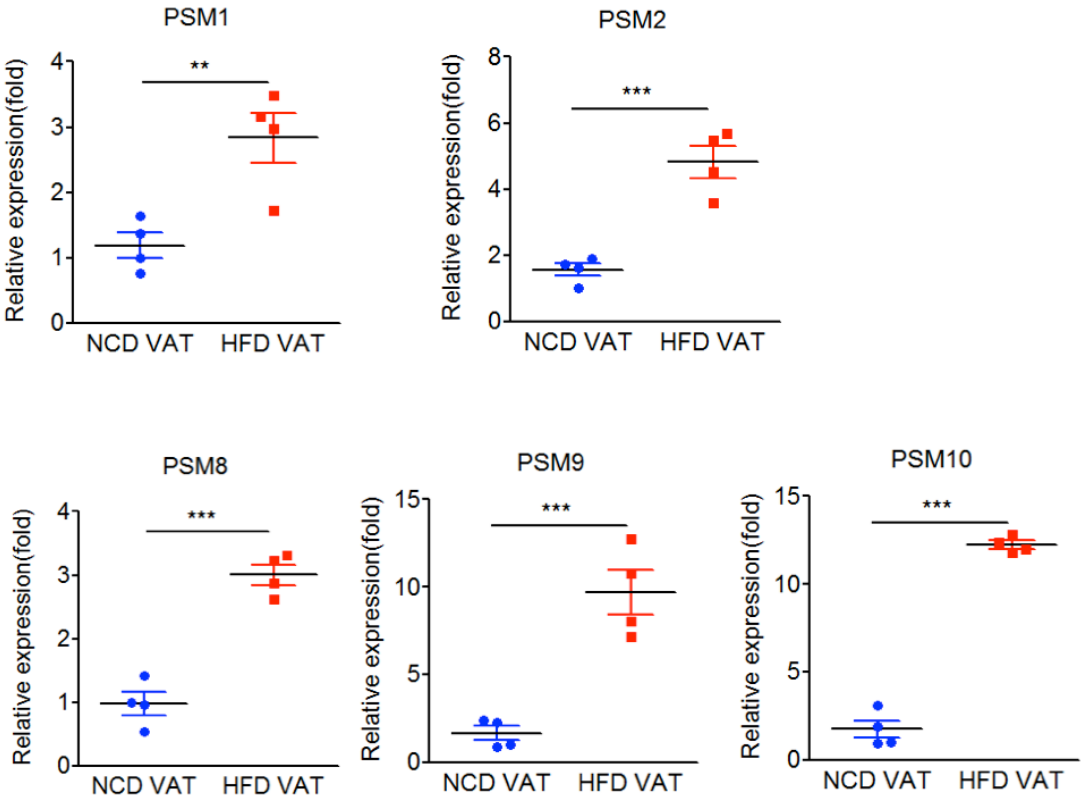


**Figure S5. The mRNA expression of proteasomes (PSM1/2) and immunoproteasomes (PSM8/9/10) is increased in obese visceral adipose tissues, Related to Figure 6**

Quantitative real-time PCR analysis of the mRNA expression of proteasomes (PSM1/2) and immunoproteasomes (PSM8/9/10) catalytic subunits in the epididymal fat pads from mice after 4-week NCD or HFD feeding (4 mice per group) Data are means and error bars are ±SEM.

* $p < 0.05$, ** $p < 0.01$,and *** $p<0.0001$, determined by Student's t-test.

**Table S3. The exclusive high confidence H2-Kb-bound peptides from visceral adipose tissues of HFD-fed mice, Related to Figure 2**

| HFD VAT-exclusive MIP | Sequence | Length | Charge | MH+ [Da] | ΔM [ppm] | RT [min] | Proteins | Protein Accessions | Mascot IonScore | Sequest q-Value | MHC binding Affinity ($IC_{50}$ nM) |
|---|---|---|---|---|---|---|---|---|---|---|---|
| 1. | AALIYTSV | 8 | 1 | 837.4681 | -4.22 | 32 | 2 | Q6PDL0,Q8R1Q8 | 31 | | 67.9 |
| 2. | AAVKFHNL | 8 | 2 | 899.5085 | -1.48 | 13.39 | 1 | Q64521 | 26 | | 15.8 |
| 3. | AAYEFTTL | 8 | 1 | 915.4449 | -1.06 | 36.61 | 1 | P32233 | 25 | | 3.3 |
| 4. | ANVQYMRV | 8 | 2 | 980.496 | -2.34 | 18.99 | 1 | Q61805 | 34 | | 31.8 |
| 5. | ASTIAYLAL | 9 | 2 | 922.5235 | -1.04 | 28.57 | 1 | O70503 | 28 | | 252.5 |
| 6. | ASVVFNQL | 8 | 2 | 877.477 | -0.9 | 18.86 | 1 | Q64288 | 25 | | 10.9 |
| 7. | ATLRYASL | 8 | 2 | 894.5022 | -2.45 | 21.8 | 1 | Q9DBR4 | 23 | | 3.9 |
| 8. | DFFNYAGL | 8 | 1 | 946.4321 | 1.68 | 33.05 | 1 | P12265 | 27 | | 43.4 |
| 9. | FAASYSAL | 8 | 1 | 829.4089 | -0.24 | 28.48 | 1 | Q8BFW3 | 22 | | 81.8 |
| 10. | GQYEFHSL | 8 | 2 | 980.4457 | -1.55 | 23.22 | 1 | Q61805 | 33 | | 91.9 |
| 11. | IGPYFEHNM | 9 | 2 | 1107.491 | -1.53 | 25.46 | 1 | Q8VCB3 | 24 | | 60.6 |
| 12. | ISDVRVTQL | 9 | 2 | 1030.586 | -3.22 | 31.18 | 1 | P55065 | 22 | | 355.6 |
| 13. | KSYDMSQV | 8 | 2 | 957.4305 | -4.36 | 27.95 | 1 | Q8C8J0 | 21 | | 199.4 |
| 14. | KSYLMNKL | 8 | 2 | 996.5522 | -2.54 | 17.72 | 3 | Q01514,Q8CFB4, Q9Z0E6 | 28 | | 29.4 |
| 15. | KVYTFNSV | 8 | 2 | 957.5032 | -0.91 | 21.38 | 3 | G5E829,Q6Q477, Q9R0K7 | 27 | | 10.5 |
| 16. | LAAQFSQL | 8 | 2 | 877.477 | -0.9 | 18.86 | 1 | Q9DCB4 | 31 | | 62 |
| 17. | LAPVYQRL | 8 | 2 | 959.5665 | -0.89 | 22.4 | 1 | P82198 | 26 | | 17.7 |
| 18. | NSFRYNGL | 8 | 2 | 970.4738 | -0.34 | 21.83 | 1 | P41105 | 21 | | 9.3 |
| 19. | QNYTYSSL | 8 | 1 | 975.4399 | -1.91 | 26.3 | 1 | Q810S1 | 21 | | 3.9 |

| | | | | | | | | | | | |
|---|---|---|---|---|---|---|---|---|---|---|---|
| 20. | RSYDFEFM | 8 | 2 | 1094.459 | -1.76 | 35.43 | 1 | P40336 | 21 | | 21.5 |
| 21. | SAPQFSKL | 8 | 2 | 877.4777 | -0.21 | 18.92 | 1 | Q8K007 | 28 | | 13.9 |
| 22. | SAPQYSRL | 8 | 2 | 921.4781 | -0.88 | 14.1 | 1 | Q8CFG0 | 24 | | 8.1 |
| 23. | SAYQRGESL | 9 | 2 | 1010.488 | -2.32 | 12.24 | 1 | O35382 | 26 | | 233.2 |
| 24. | SGLKYVNV | 8 | 2 | 879.4932 | -0.3 | 20.85 | 1 | Q8VCP8 | 26 | | 14.6 |
| 25. | SGLVYKNV | 8 | 2 | 879.4922 | -1.47 | 20.64 | 1 | Q80TI1 | 26 | | 30.4 |
| 26. | SGNIFVASL | 9 | 2 | 907.4867 | -1.83 | 27.44 | 1 | O88495 | 25 | | 35.8 |
| 27. | SIVSYNHL | 8 | 2 | 932.4822 | -1.5 | 22.3 | 1 | Q9JHU9 | 21 | | 10.2 |
| 28. | SNPEFRQL | 8 | 2 | 990.4994 | -0.99 | 18.61 | 1 | Q3UWM4 | 27 | | 17.3 |
| 29. | SSGDFPSL | 8 | 1 | 809.3663 | -1.58 | 32.32 | 1 | Q9WVK4 | 24 | | 138.2 |
| 30. | SSYNYRVV | 8 | 2 | 987.4875 | -1.98 | 18.4 | 1 | P11881 | 26 | | 5.4 |
| 31. | STFSFTKV | 8 | 2 | 916.4765 | -1.09 | 25.63 | 1 | Q3TZZ7 | 21 | | 7.7 |
| 32. | TTYKYEMI | 8 | 2 | 1048.502 | -0.21 | 24.58 | 1 | Q8QZY1 | 28 | | 28.6 |
| 33. | VFTEVANL | 8 | 1 | 892.4758 | -1.94 | 34.23 | 1 | Q62141 | 22 | | 195.2 |
| 34. | VFYEREVQM | 9 | 2 | 1200.569 | -2.64 | 25.49 | 1 | Q80SY3 | 31 | | 86.2 |
| 35. | VGINYREV | 8 | 2 | 949.5077 | -2.65 | 20.47 | 1 | Q01320 | 22 | | 46.2 |
| 36. | VNFEFPEF | 8 | 2 | 1028.47 | -1.98 | 50.37 | 1 | P62082 | 22 | | 43.3 |
| 37. | VNILENYL | 8 | 2 | 977.5284 | -1.93 | 31.24 | 1 | Q64435 | 22 | | 402.5 |
| 38. | VNIQYEVI | 8 | 2 | 977.5284 | -1.93 | 31.24 | 1 | Q60961 | 25 | | 324.5 |
| 39. | VNIQYLDL | 8 | 2 | 977.529 | -1.24 | 31.14 | 1 | Q8R0G9 | 21 | | 17 |
| 40. | AIYAFSHL | 8 | 2 | 921.482 | -1 | 30.93 | 1 | Q9JJ59 | | 0 | 2.2 |
| 41. | GTYDYTQL | 8 | 1 | 960.4302 | -0.77 | 30.12 | 1 | Q8K2A8 | | 0 | 31.7 |
| 42. | RAPVYARI | 8 | 2 | 945.5602 | -2.83 | 13.58 | 1 | P52840 | | 0 | 25 |
| 43. | RAYLFAHV | 8 | 2 | 976.5349 | -1.48 | 22.42 | 1 | Q5SWD9 | | 0 | 2.5 |
| 44. | RVYEFTRA | 8 | 2 | 1041.546 | -1.74 | 13.38 | 1 | Q8VI38 | | 0.049 | 45.2 |
| 45. | SGYDYYHV | 8 | 2 | 1003.415 | -0.8 | 22.78 | 1 | O08785 | | 0 | 6.9 |

| | | | | | | | | | | | |
|---|---|---|---|---|---|---|---|---|---|---|---|
| 46. | SQYRFEHL | 8 | 2 | 1079.525 | -1.46 | 17.98 | 1 | Q3UJK4 | | 0 | 3.8 |
| 47. | SSPKFSEI | 8 | 2 | 894.4559 | -1.01 | 18.91 | 1 | Q91VM3 | | 0 | 53.5 |
| 48. | AAYGFRNI | 8 | 2 | 911.4717 | -1.91 | 23.04 | 1 | Q9CYQ7 | 30 | 0 | 9.6 |
| 49. | IGPRYSSV | 8 | 2 | 878.4706 | -2.85 | 15.19 | 1 | Q5PRF0 | 26 | 0 | 19.4 |
| 50. | SAPLYTNL | 8 | 1 | 878.46 | -2.13 | 31 | 1 | Q8K4S1 | 25 | 0 | 4.6 |
| 51. | SAYEVIKL | 8 | 2 | 922.5235 | -1.04 | 28.57 | 2 | P06151,P16125 | 38 | 0 | 56.8 |
| 52. | STFVYNTM | 8 | 1 | 962.4263 | -2.65 | 29.89 | 1 | Q8CFB4 | 38 | 0 | 7.7 |
| 53. | **SAYEFYHA** | **8** | **2** | **987.4195** | **-1.22** | **22.43** | **1** | **P97481** | **26** | | **13** |
| 54. | **SGTQYFRV** | **8** | **2** | **957.477** | **-1.99** | **19.42** | **1** | **P97412** | **21** | | **201.2** |
| 55. | **SLYQPAGL** | **8** | **1** | **848.4503** | **-1.12** | **31** | **1** | **P19096** | **40** | | **70.7** |
| 56. | **SSPHYTTL** | **8** | **2** | **905.4344** | **-2.16** | **14.13** | **1** | **P27046** | | **0** | **12.2** |
| 57. | **STTVFHSL** | **8** | **2** | **891.4551** | **-2.26** | **21.06** | **1** | **P19096** | | **0** | **44.2** |

Note: five of the peptides highlighted in red color did not display HFD VAT MIP specificity at the source protein level.

**Table S4. Peptides and their potential source proteins found to be exclusively expressed in VAT MIP from HFD-induced obese mice as described in Section 2, Related to Figure 2**

| Peptide | | | Source Protein | | |
|---|---|---|---|---|---|
| Sequence | Length | Affinity( nM) | Accession No | Name | Peptide Position |
| | | | | Proteins involved in Glucose metabolism | |
| AAVKFHNL | 8 | 15.8 | Q64521 | Glycerol-3-phosphate dehydrogenase 2 | 450-457 |
| DFFNYAGL | 8 | 43.4 | P12265 | Beta-glucuronidase | 206-213 |
| IGPYFEHNM | 9 | 60.6 | Q8VCB3 | Glycogen synthase 2 | 66-74 |
| SAYEVIKL | 8 | 56.8 | P06151 | L-lactate dehydrogenase A chain | 237-244 |
| | | | P16125 | L-lactate dehydrogenase B chain | 238-245 |
| | | | | Proteins involved in lipid metabolic process | |
| ASTIAYLAL | 9 | 252.5 | O70503 | 17-beta-hydroxysteroid dehydrogenase 12 | 16-24 |
| ISDVRVTQL | 9 | 355.6 | P55065 | Phospholipid transfer protein | 65-73 |
| RAPVYARI | 8 | 25 | P52840 | Sulfotransferase 1A1 | 68-75 |
| RVYEFTRA | 8 | 45.2 | Q8VI38 | Forssman glycolipid synthase | 271-278 |
| SAPLYTNL | 8 | 4.6 | Q8K4S1 | Phosphoinositide phospholipase C-epsilon-1 | 1232-1239 |
| SIVSYNHL | 8 | 10.2 | Q9JHU9 | Inositol-3-phosphate synthase 1 | 328-335 |
| STFSFTKV | 8 | 7.7 | Q3TZZ7 | Extended synaptotagmin-2 | 157-164 |
| | | | | Proteins involved in protein metabolism | |
| AAYEFTTL | 8 | 3.3 | P32233 | Developmentally-regulated GTP-binding protein 1 | 92-99 |
| NSFRYNGL | 8 | 9.3 | P41105 | 60S ribosomal protein L28 | 36-43 |
| SNPEFRQL | 8 | 17.3 | Q3UWM4 | Lysine-specific demethylase 7A | 775-782 |
| SQYRFEHL | 8 | 3.8 | Q3UJK4 | GTP-binding protein 2 (GTP-binding-like protein 2) | 78-85 |
| SSPKFSEI | 8 | 53.5 | Q91VM3 | WD repeat domain phosphoinositide-interacting protein 4 | 70-77 |
| TTYKYEMI | 8 | 28.6 | Q8QZY1 | Eukaryotic translation initiation factor 3 subunit L | 353-360 |

| | | | | | |
|---|---|---|---|---|---|
| VFTEVANL | 8 | 195.2 | Q62141 | Paired amphipathic helix protein Sin3b | 205-212 |
| VNFEFPEF | 8 | 43.3 | P62082 | 40S ribosomal protein S7 | 185-192 |
| | | | | Proteins involved in establishment of localization | |
| AIYAFSHL | 8 | 2.2 | Q9JJ59 | ATP-binding cassette sub-family B member 9 | 23-30 |
| IGPRYSSV | 8 | 19.4 | Q5PRF0 | HEAT repeat-containing protein 5A | 1980-1987 |
| | | | Q6Q477 | Plasma membrane calcium-transporting ATPase 4 | 565-572 |
| KVYTFNSV | 8 | 10.5 | Q9R0K7 | Plasma membrane calcium-transporting ATPase 2 | 553-560 |
| | | | G5E829 | Plasma membrane calcium-transporting ATPase 1 | 574-581 |
| LAPVYQRL | 8 | 17.7 | P82198 | Transforming growth factor-beta-induced protein ig-h3 | 670-677 |
| QNYTYSSL | 8 | 3.9 | Q810S1 | Calcium uniporter regulatory subunit MCUb | 281-288 |
| RSYDFEFM | 8 | 21.5 | P40336 | Vacuolar protein sorting-associated protein 26A | 105-112 |
| VFYEREVQM | 9 | 86.2 | Q80SY3 | V-type proton ATPase subunit d 2 | 292-300 |
| VNIQYLDL | 8 | 17 | Q8R0G9 | Nuclear pore complex protein Nup133 | 337-344 |
| | | | | Proteins involved in response to stimulus | |
| AALIYTSV | 8 | 67.9 | Q6PDL0 | Cytoplasmic dynein 1 light intermediate chain 2 | 267-274 |
| | | | Q8R1Q8 | Cytoplasmic dynein 1 light intermediate chain 1 | 280-287 |
| ANVQYMRV | 8 | 31.8 | Q61805 | Lipopolysaccharide-binding protein | 474-481 |
| GQYEFHSL | 8 | 91.9 | | | 74-81 |
| ASVVFNQL | 8 | 10.9 | Q64288 | Olfactory marker protein | 156-163 |
| ATLRYASL | 8 | 3.9 | Q9DBR4 | Amyloid-beta A4 precursor protein-binding family B member 2 | 387-394 |
| FAASYSAL | 8 | 81.8 | Q8BFW3 | Protein phosphatase 1 regulatory subunit 15B | 93-100 |
| KSYLMNKL | 8 | 29.4 | Q8CFB4 | Guanylate-binding protein 5 | 51-58 |
| STFVYNTM | 8 | 7.7 | | | 124-131 |
| LAAQFSQL | 8 | 62 | Q9DCB4 | cAMP-regulated phosphoprotein 21 | 547-554 |
| SAPQFSKL | 8 | 13.9 | Q8K007 | Extracellular sulfatase Sulf-1 | 230-237 |
| SAPQYSRL | 8 | 8.1 | Q8CFG0 | Extracellular sulfatase Sulf-2 | 231-238 |

| | | | | | |
|---|---|---|---|---|---|
| SAYQRGESL | 9 | 233.2 | O35382 | Exocyst complex component 4 | 322-330 |
| SGNIFVASL | 9 | 35.8 | O88495 | G protein-coupled receptor 50 | 70-78 |
| SGYDYYHV | 8 | 6.9 | O08785 | Circadian locomoter output cycles protein kaput | 308-315 |
| SSGDFPSL | 8 | 138.2 | Q9WVK4 | EH domain-containing protein 1 | 349-356 |
| SSYNYRVV | 8 | 5.4 | P11881 | Inositol 1,4,5-trisphosphate receptor type 1 | 1169-1176 |
| VGINYREV | 8 | 46.2 | Q01320 | DNA topoisomerase 2-alpha | 67-74 |
| VNILENYL | 8 | 402.5 | Q64435 | UDP-glucuronosyltransferase 1-6 | 214-221 |
| | | | | Others | |
| AAYGFRNI | 8 | 9.6 | Q9CYQ7 | Nuclear prelamin A recognition factor | 351-358 |
| GTYDYTQL | 8 | 31.7 | Q8K2A8 | Dol-P-Man:Man(5)GlcNAc(2)-PP-Dol alpha-1,3-mannosyltransferase | 84-91 |
| KSYDMSQV | 8 | 199.4 | Q8C8J0 | Sperm-tail PG-rich repeat-containing protein 2 | 431-438 |
| RAYLFAHV | 8 | 2.5 | Q5SWD9 | Pre-rRNA-processing protein TSR1 homolog | 250-257 |
| SGLKYVNV | 8 | 14.6 | Q8VCP8 | Adenylate kinase isoenzyme 6 | 27-34 |
| SGLVYKNV | 8 | 30.4 | Q80TI1 | Pleckstrin homology domain-containing family H member 1 | 460-467 |
| VNIQYEVI | 8 | 324.5 | Q60961 | Lysosomal-associated transmembrane protein 4A | 60-67 |

Note: peptides sequence, length, predicted H2-Kb-binding affinity ($IC_{50}$), protein name, accession number and function, according to Uniprot database are listed.

**Table S5. Several known obesity-associated proteins are detected in the obese VAT-exclusive MIPs source proteome, Related to Figure 2**

| Protein ID | Protein name (gene) | Functions | Obesity-association | References |
|---|---|---|---|---|
| Q61805 | Lipopolysaccharide-binding protein (Lbp) | Lipid binding | LBP is an inflammatory marker associated with obesity-related insulin resistance | (Kim et al., 2016; Moreno-Navarrete et al., 2012) |
| O88495 | Melatonin-related receptor (Gpr50) | G-protein coupled receptor activity; regulating energy metabolism | GPR50 knockout mice were partially resistant to diet-induced obesity. | (Ivanova et al., 2008). |
| P55065 | Phospholipid transfer protein (Pltp) | lipid transporter activity | PLTP mass and activity have been found to be elevated in the plasma of type 2 diabetes mellitus (T2DM) and obese patients.<br>PLTP mass and activity have been found to be positively associated with BMI, fat mass and leptin levels.<br>PLTP activity is independently associated with nonalcoholic fatty liver disease. | (Qin et al., 2014)<br>(Tzotzas et al., 2009) |
| Q8VCB3 | Glycogen synthase 2 (Gys2) | Glucose binding | GYS2 as a novel genetic factor for polycystic ovary syndrome through obesity-related condition. | (Hwang et al., 2012) |

| | | | | |
|---|---|---|---|---|
| Q8CFG0 | Extracellular sulfatase Sulf-2 (Sulf2) | arylsulfatase activity | SULF2 strongly predisposes to fasting and postprandial triglycerides in patients with obesity and type 2 diabetes mellitus. | (Hassing et al., 2014) |
| P06151 | L-lactate dehydrogenase A chain (Ldha) | pyruvate fermentation to lactate | Lactate dehydrogenase gene is downregulated in visceral white adipose tissue of HFD-fed rats, suggesting a decreased anaerobic degradation of glucose in adipose tissue. As a result, pyruvate would be directed to acetyl-CoA production, which in turn would fuel fatty acid biosynthesis and triglyceride storage. However, it has also been reported that activating or overexpressing LDH-A react against lipid accumulation by deviating pyruvate to lactate. Lactate increases the destiny of white adipose cells towards a brown phenotype. The elevated level of LDHA has been suggested to be related with the reduction of body weight gain. | (Lopez et al., 2004; Parray and Yun, 2015) |
| Q64521 | Glycerol-3-phosphate dehydrogenase 2, mitochondrial (Gpd2) | Calcium ion binding; gluconeogenesis; NADH metabolic process | Mitochondrial glycerol 3-phosphate dehydrogenase (mGPDH) is an integral component of the respiratory chain.<br>Lou/C, a rat strain derived from Wistar, is resistant to age- and diet-related obesity, and this feature has been shown to be linked to a high expression and activity of mitochondrial glycerol-3-phosphate dehydrogenase.<br>Deficiency of the mitochondrial glycerol 3-phosphate dehydrogenase contributes to hepatic steatosis. | (Taleux et al., 2009)<br>(Zheng et al., 2019) |

**Table S6. Selected potential candidate peptides for immunogenicity evaluation, Related to Figure 3 and Figure 4**

| Group | Name | Source protein | Protein_ID | Function | Sequence | IC50(nM) | HFD-VAT MIP | NCD-VAT MIP |
|---|---|---|---|---|---|---|---|---|
| G1 | $DHB_{16-24}$ | 17-beta-hydroxys-teroid dehydrogenase 12 | O70503 | Oxidoreductase; lipid metabolism | ATLRYASL | 252.2 | + | - |
| | $LBP_{74-81}$ | Lipopolysaccharide-binding protein | Q61805 | Lipid binding; immune system process; response to stimulus | GQYEFHSL | 91.9 | + | - |
| | $LDHA_{237-244}$ | L-lactate dehydrogenase A or B chain | P06151 | Oxidoreductase; glucose metabolism; response to stimulus | SAYEVIKL | 56.8 | + | - |
| | $APBB2_{387-394}$ | Amyloid-beta A4 precursor protein-binding family B member 2 | Q9DBR4 | Nucleic acid-templated transcription; response to stimulus | ATLRYASL | 3.9 | + | - |
| | $V\text{-}ATPase_{292-300}$ | V-type proton ATPase subunit d 2 | Q80SY3 | Hydrolase | VFYEREVQM | 86.2 | + | - |

| | | | | | | | | |
|---|---|---|---|---|---|---|---|---|
| G2 | ITPR1$_{1169-1176}$ | Inositol 1,4,5-trisphosphate receptor type 1 | P11881 | Calcium ion transport | SSYNYRVV | 5.4 | + | - |
| | EXOC4$_{322-330}$ | Exocyst complex component 4 | O35382 | Golgi to plasma membrane transport | SAYQRGESL | 233.2 | + | - |
| | GBP5$_{124-131}$ | Guanylate-binding protein 5 | Q8CFB4 | GTPase activity | STFVYNTM | 7.7 | + | - |
| | AK6$_{10-17}$ | Adenylate kinase isoenzyme 6 | Q8VCP8 | ATPase activity | SGLKYVNV | 14.6 | + | - |
| | EHD1$_{349-356}$ | EH domain-containing protein 1 | Q9WVK4 | ATP/GTP binding; calcium ion binding | SSGDFPSL | 138.2 | + | - |
| G3 | CATA$_{384-392}$ | Catalase | P24270 | Cholesterol metabolic process | ANYQRDGPM | 214.7 | +++ | + |
| | PLIN2$_{213-221}$ | Perilipin-2 | P43883 | Lipid storage; long-chain fatty acid transport | SNYERLESL | 64.4 | +++ | + |
| | D19L3$_{433-440}$ | Probable C-mannosyltransferase DPY19L3 | Q71B07 | Transferase activity | SVVAFHNL | 8.69 | +++++++ | + |

Note: a plus or multiple plus indicates the abundance of the indicated peptide in the given tissue-derived MIP; the minus sign indicates that the indicated peptide cannot be detected in the given tissue-derived MIP.

## Transparent Methods

### Animal models

Four-week-old male C57BL/6J wild-type mice (HFK Bioscience, Beijing, China) were maintained under a 12 h light-dark cycle in specific pathogen-free facilities, and were allowed free access to sterilized water and to either a high fat diet (HFD, D12492, 60 Kcal% fat, Research Diets) or a normal chow diet (NCD, D12450B 10 Kcal% fat, Research Diets). For the glucose tolerance test (GTT), the mice were made to fast for 16 h prior to intraperitoneal administration of glucose (1g $kg^{-1}$). Blood glucose was measured from tail vein at indicated time points with a glucometer (ONETOUCH Ultra). For the insulin tolerance test (ITT), mice were made to fast for 4 h prior to intraperitoneal administration of insulin (Novolin; 0.75U $kg^{-1}$) and blood glucose concentrations were measured at indicated time points. All procedures were approved by the Institute Animal Care and Use Committee of the Third Military Medical University (Chongqing, China).

### Isolation of MIP from VAT

The epididymal fat pad (VAT samples) (total 28 g) were collected from 25 HFD-fed obese male mice or 75 NCD-fed lean male mice at 12 weeks of age from three different batches, respectively, and immediately lysed in 40 ml of ice-cold lysis buffer (50 mM Tris-HCl, 150 mM NaCl, and 1% of CHAPS, pH 8.0) containing “complete” protease inhibitor (Roche). Cell lysates were clarified by several rounds of centrifugation (12000g, 30 min, 4°C), and the supernatant was collected and used for immunoaffinity chromatography. The MIPs were isolated following a method described previously (Delgado et al., 2009; Escobar et al., 2008; Purcell, 2004) with some modifications. Initially, immunoaffinity columns were constructed

based on the following steps: 1) the top-cap of 1 ml HiTrap NHS-activated HP column (Code No:17-0716-01, GE Healthcare) was removed and a drop of ice-cold 1 mM HCl was introduced into the top to avoid air bubble formation; 2) 3 × 2 ml ice-cold 1 mM HCl was injected to wash out the isopropanol in the column at a flow rate not exceeding 1 ml/min. 3) For antibody coupling, 10 ml of 1 mg/ml anti-H2-Kb mAb (clone: Y-3, Bioxcell company) antibody in coupling buffer (0.2 M NaHCO3, 0.5 M NaCl, pH 8.3) was passed through the column repeatedly at a flow rate of 1 ml/min for 4 h at 4 °C. 4) To deactivate any excess active groups that had not coupled to the ligand and to wash out the non-specifically bound ligands, 3 × 2 ml of Buffer A (0.5 M ethanolamine, 0.5 M NaCl, pH 8.3) and 3 × 2 ml of Buffer B (0.1 M sodium acetate, 0.5 M NaCl, pH 4) were injected into the column alternately; after the columns were maintained at room temperature for 15–30 min, 3 × 2 ml of Buffer B and 3 × 2 ml of Buffer A were injected into the column alternately; 15 ml of lysis buffer (50 mM Tris-HCl, pH 8.0 150 mM NaCl and 1% of CHAPS) was injected into the column. Next, the VAT proteolytic solution was repeatedly circulated in the column overnight at a flow rate of 1 ml/min at 4°C. Following this, the column was washed with several buffers in the following order: 15 ml of wash buffer 1 ( 50 mM Tris-HCl, pH 8.0, 150 mM NaCl, and 1% of CHAPS), 15 ml of wash buffer 2 (50 mM Tris-HCl, pH 8.0, 150 mM NaCl in deionized $H_2O$), 25 ml of wash buffer 3 (50 mM Tris-HCl, pH 8.0, 450 mM NaCl in deionized $H_2O$), and 35 ml of wash buffer 4 (50 mM Tris-HCl, pH 8.0, in deionized $H_2O$). Subsequently, the HLA-peptide complexes were eluted with 6 ml of 10% acetic acid. The ultrafiltration filters (3.0-kDa cutoff Microcon, Millipore) were prewashed with 0.1 N acetic acid and 10% acetonitrile to remove contaminants interfering with the mass spectrometry, and the mixture of peptides and class I heavy-chain and β2-microglobulin were

separated by ultrafiltration at 10000 × g (Escobar et al., 2008; Murphy et al., 2017). After ultrafiltration, the peptides mixtures were desalinated and concentrated by Micro-Tip reversed-phase C18 columns (Merck) (Bassani-Sternberg et al., 2010). The C18 columns were washed with 80% acetonitrile in 0.1% TFA, equilibrated with 0.1% TFA, and loaded with the peptide mixture. The C18 columns were washed additionally by 0.1% TFA. Lastly, the peptides were eluted with 400 μl 80% acetonitrile in 0.1% TFA, and all peptide elutions were vacuum concentrated to a final volume of 20 μl prior to mass spectrometry analysis.

**MIP analysis using LC-MS/MS**

MIP samples were loaded into an analytical column (Acclaim™ PepMap™ 100, 75 μm ×15 cm, C18, 3 μm, 100 Å, Thermo Fisher Scientific) with a Trap Column (Acclaim™ PepMap™ 100, 75 μm×2 cm, C18, 3 μm, 100 Å, Thermo Fisher Scientific) and separated by reversed-phase chromatography (Easy nanoLC1000, Thermo Fisher Scientific) using a 120 min gradient at a flow rate of 300 nL/min. The gradient was composed of Solvent A (0.1% formic acid in water) and Solvent B (0.1% formic acid in acetonitrile); the elution gradient was as follows: 2-7% B in 3 min, 7-22% B in 96 min, 22-35% B in 10 min, 35-90% B in 2 min, 90% B for 5 min and 90-2% B in 2 min, 2% B for 2 min. The eluted peptides were sprayed into the LTQ Orbitrap using nano-electron spray ionization (NSI) at a capillary voltage of 2.5 KV and 300 ℃capillary temperature. The instrument was operated in the data-dependent mode. Survey MS spectra from 350.0–1800.0 m/z were obtained in the orbitrap at 60,000 M/ΔM resolution, followed by data dependent acquisition (DDA) of the top 16 most abundant precursor ions with an isolation window of 2.0 m/z, and followed by MS/MS scans of the ion trap using product ion scans (relative CID energy 35) of the top 16 most abundant precursor ions in the survey scan. MS

scans were captured in profile mode, while the MS/MS scans was captured in centroid mode. The product ion scans were obtained using a 2.0-unit isolation width and normalized collision energy of 35 in an LTQ Orbitrap Velos Pro MS spectrometer (Thermo Fisher Scientific). Three replicate injections were performed for each set of samples.

**Database search and spectral annotation**

Acquired tandem mass spectrometric spectra were searched using Mascot (version 2.3, Matrix Science) and the Sequest HT search engine with the Proteome Discoverer software (PD) (version 1.4.0.288, Thermo Fisher Scientific) against the UniProt mouse FASTA protein database and reversed decoy sequences. MS/MS spectra were captured in CID mode. Mascot search parameters were set as follows: precursor ion mass tolerance 5 ppm, fragment ion mass tolerance 0.8Da, no enzyme specificity, oxidized methionine was allowed as a dynamic modification, FDR<5% (peptide-spectrum match level). Protein grouping was disabled, allowing multiple annotations of peptides (for example, conserved sequence mapping into multiple proteins). The Sequest HT used the same search parameters as Mascot. Mascot and Sequenst search results in technical triplicates were combined to establish datasets of HFD VAT MIP and NCD VAT MIP. Firstly, peptides with either an Ionscore>20 in Mascot search (Al-Shahib et al., 2010; Kowalewski and Stevanovic, 2013; Kumar et al., 2015; Ni et al., 2019) or a q-value<0.05 in Sequest search (Franchin et al., 2014; Kall et al., 2008) were collected. Secondly, peptide lengths were limited to 8-12 amino acids. Finally, high confidence H2-Kb-associated peptides were identified by $IC_{50}$<500 nM (NetMHC 4.0: http://www.cbs.dtu.dk/services/NetMHC/), (Andreatta and Nielsen, 2016)

**Determination of MHC class I motifs**

We used the weblogo program (http://weblogo.berkeley.edu/logo.cgi) to visualize the characteristics of the binding motifs. The information content at each position in the sequence motif corresponds to the height of a column of letters. The height of each letter within the column is proportional to the frequency of the corresponding amino acid at that position.

**Annotation enrichment analysis and functional annotation of MIP source proteins**

Biological annotation and KEGG pathway enrichment of the VAT MIP source proteins was performed using the R package “clusterProfiler” (version 3.10.1).Terms with adjusted P value < 0.01 were considered significant.

**Peptide Synthesis**

The peptides were synthesized at a purity>95% at the Chinese Peptide Company (Hangzhou, China). Synthetic peptides were used for validation of LC-MS/MS identification as well as for functional experiments.

**H2-Kb binding assays**

Peptide binding to H2-Kb was measured using the transporter associated with TAP-deficient RMAS cell line. Briefly, RMAS cells were cultured overnight in complete medium at 26 °C, 5% $CO_2$. The RMAS cells ($1x10^6$ cells/ml) were incubated with or without each peptide pool (total 100 μg/ml) for 3 h at 26 °C, followed by a second incubation for 3 h at 37 °C, 5% $CO_2$. An H2-Kb-binding LCMV peptide $GP_{33-41}$ (KAVYNFATM) was used as a positive control. After incubation, the cells were washed twice with ice-cold PBS and stained with PE-conjugated anti-mouse H2-Kb mAb (eBioscience, AF6) for 30 min at 4 °C. The cells were washed and detected by flow cytometry (BD FACS Calibur). Data analysis was performed using the FlowJo software (v7.6.3, Treestar, San Carlos, CA, USA).

**Amplification of Peptide-Specific $CD8^+$T Cells and intracellular cytokine staining**

Splenocytes isolated from C57BL/6J mice were stimulated with each peptide pool or single peptide (100 μg/ml) in complete medium containing recombinant IL-2 (30 IU/ml; Roche), and half the medium was replaced with complete medium supplemented with IL-2 every 3–4 days. Cell cultures were restimulated with the peptide pool or single peptide (50 μg/ml)-pulsed RMAS cells or only RMAS cells on day 7. To block the H2-Kb-restricted recognition of $CD8^+$ T cells, anti-H2-Kb antibody Y-3 (10 μg/ml) was added to the cell cultures. The presence of peptide-specific $CD8^+$ T cells was assessed by intracellular IFN-γ and TNF-α staining. Two hours after the restimulation, 0.65μl $ml^{-1}$GolgiStop™ (BD Biosciences) was added into each culture at 37 °C and incubated for an additional 4 hours. Before staining, all cell preparations were incubated with anti-mouse CD16/32 (BD Biosciences) for 10 min on ice to block the Fc receptors. Dead cells were excluded from the analysis by using the fixable Viability Dye eFluor® 780 (eBioscience). Percp-cy5.5-conjugated CD3 mAb (clone:53-6.7 eBioscience) and FITC-conjugated anti-CD8α mAb (clone:17A2 eBioscience) were used to label cells for 30 min on ice. After washing with the flow cytometer buffer (PBS/1% FBS), cells were fixed and then labeled with PE-conjugated anti-mouse TNF-α (clone: MP6-XT22 eBioscience) or APC-conjugated anti-mouse IFN-γ (clone: XMG1.2 eBioscience) at 4 °C in a permeabilization buffer. PE or APC-conjugated isotype IgG1 was used as a negative staining control (eBioscience). Flow cytometry data were acquired for each of the experiments using a BD FACS Calibur (BD Biosciences, Franklin Lakes, NJ). Data analysis was performed using the FlowJo software.

**Pentamer staining**

Lymphocytes were isolated from the mesenteric lymph nodes of HFD-fed obese mice and NCD-fed lean mice post the 8-week feeding. A single cell suspension was prepared in PBS at a cell concentration of 1-2·$10^6$ cells/100 μl, initially stained with Fixable Viability Dye eFluor® 780 (eBioscience) and washed, and then stained with PE-conjugated pentamers (Proimmune,5 μl/test) for 15 min-incubation at 37 ºC in dark. After washing twice with FACS buffer, cells were incubated with FITC-conjugated-anti-mouse CD8 (clone: 17A2, eBioscience) at 4 ºC for 30 min. Cells were washed twice with FACS buffer, and fixed with 1% polyformaldehyde. After washing, stained cells were resuspended in 200-300 μl FACS buffer and measured using a BD FACS Calibur (BD Biosciences, Franklin Lakes, NJ).

**Preparation of VAT-isolated stromal-vascular fractions (SVF)**

Acquired epididymal VAT from HFD-fed obese mice and NCD-fed lean mice were divided into fine pieces in a weight boat containing 3 ml DPBS supplemented with 0.5% BSA. The VAT samples were then poured into 50 ml conical tubes, rinsed with 3 ml collagenase II digest solution consisting of 1X DPBS supplemented with 0.5% BSA, 10 mM CaCl2, and 4 mg/ml type II collagenase, and incubated in a rotational shaker (200 rpm, 37 ºC, 20 min). The VAT homogenate, along with 10 ml DPBS (0.5% BSA), was passed through a 100 μm filter into fresh 50 ml conical tubes. The VAT-isolated SVFs were obtained after centrifuging cell suspensions (500g, 4 ºC, 10 min) and discarding the supernatant. The VAT-isolated SVFs were restimulated with peptide (10 μg/ml)-pulsed RMAS cells or RMAS cells alone. The presence of peptide-specific $CD8^+$ T cells was assessed by intracellular IFN-γ and TNF-α staining.

**Treatment of mice**

C57BL/6J male mice administered HFD starting at 4 weeks of age were randomly divided into 4 groups (4-5 mice per group), two of which were administered 20 μg $LDHA_{237-244}$ peptide or PBS (once a day at day 1-5, 8, then once a week until the age of 12 weeks) intranasally, starting at 4 weeks of age, and the other two groups were injected intraperitoneally with 50 μg $LDHA_{237-244}$ peptide (twice a week for the first two weeks and once a week until the age of 12 weeks) or PBS simultaneously. Weight changes were monitored weekly until 12 weeks of age. GTT and ITT were measured at 12 weeks of age.

**RNA Isolation and Quantitative Real-Time PCR**

For real-time PCR, total RNA was extracted from 0.2 mg VAT using HiPure Universal RNA Kit(Magen company, Guangzhou, China). Real-time quantitative PCR was performed using TB Green™ Premix Ex Taq™ II (Tli RNaseH Plus) (Takara, Kyoto, Japan) for H2-Kb and TaqMan™ Gene Expression Master Mix (Applied Biosystems™, Foster City, CA, USA) for the other genes according to the manufacturer's instructions. The following primers were used: *H2-kb* (Fwd: ggctggtgaagcagagagac, Rev: cagcacctcagggtgacttt), *Ldha* (Mm01612132_g1, Thermo fisher), *Psmb1* (Mm00650840_m1, Thermo fisher), *Psmb2* (Mm00449477_m1, Thermo fisher), *Psmb8* (Mm00479004, Thermo fisher), *Psmb9* (Mm00440207, Thermo fisher), and *Psmb10* (Mm00479052_g1, Thermo fisher). Each sample run was performed in triplicate, and the relative mRNA expression levels were determined using the 2(-Delta Ct) method with *Gapdh* as the internal reference control.

**Western bolt analysis**

VAT from obese and lean mice were lysed in RIPA buffer (50 mM Tris-HCl pH 7.4, 1% Nonidet P-40,0.25% Na-deoxycholate, 150 mM NaCl, 1 mM EDTA) containing complete protease

inhibitor mixture (Roche Life Sciences), 1 mM Na3VO4 pH 9, 5 mM NaF, and 10 mM NEM (Sigma-Aldrich). H2-Kb molecules were separated from elution fractions using ultrafiltration with a 3-KDa cutoff. Samples were separated by SDS-PAGE and immunoblotted with the following primary antibodies: Rabbit polyclonal to MHC Class I H2-Kb (ab93364, Abcam), Rabbit monoclonal to mouse LDHA (ab101562, Abcam), and anti-mouse GAPDH antibody (ab181602, Abcam). After incubation with peroxidase-coupled secondary antibodies for 60 min, the immunocomplexes were visualized using a chemiluminescence reagent (Amersham, Freiburg, Germany), and the autoradiographs were scanned by an imaging densitometer.

**Measurement of lactate dehydrogenase (LDH) activity**

Total LDH activity in VAT was determined using the LDH activity assay kit (MAK06, Sigma) according to the manufacturer's protocol. Briefly, fresh VAT samples (100 mg) from HFD or NCD-fed mice were homogenized rapidly on ice in 500 μl of cold LDH Assay buffer and centrifuged at 10,000 g for 15 min at 4 °C to remove any insoluble materials; the soluble fraction was used for the assay. Changes in absorbance were determined by total LDH activity at 450 nm using BIO-RAD IMark™ Microplate Reader.

**Immunoprecipitation and western blot analysis of ubiquitination**

Pooled VAT tissues (0.5mg) from three or four obese or lean mice were washed twice with ice-cold PBS and lysed in 2 ml Triton-lysis buffer (20 mM Tris-HCl, pH 7.5, 150 mM NaCl, 5 mM EDTA, 2 mM dithiothreitol, 1%Triton X-100, 1% protease inhibitor cocktail, 1 mM PMSF) in the presence or absence of 10 μM MG132 (a proteasome inhibitor). The lysates were centrifuged at 12,000 × g for 10 min at 4 °C and the supernatant was precleared with 20 μL Protein A/G PLUS-Magnetic Beads (Thermo fisher ) for 1 h at 4 °C. The lysates were

immunoprecipitated overnight with LDHA-specific rabbit polyclonal antibody (19987-1-AP, proteintech, 2 μg/test) at 4 °C, followed by incubation with protein A/G Magnetic Beads. This was followed by four washes with ice-cold lysis buffer and elution in 2X SDS sample buffer. The immunoprecipitates were boiled in 2X SDS sample buffer, resolved by SDS-PAGE, and subjected to overnight immunoblotting with specific antibodies against Lys48-specific Ubiquitin (clone: Apu2, Millipore, 1:1000) or LDHA (clone: EPR1563Y, Abcam, 1:1000) at 4 °C. Proteins were visualized using a goat anti-rabbit secondary antibody conjugated to HRP (D110058-0100, shanghai shengong company, 1:5000, 1 hour at room temperature) and a chemiluminescence detection system.

**Statistical analysis**

We used the Prism5 software (GraphPad Software) for all statistical tests. The unpaired two-group comparison was conducted using Student's t-test. Data were presented as the mean ± SD. $P<0.05$ (*), $P<0.01$ (**) and $P<0.001$(***) were considered statistically significant.

**References:**


Al-Shahib, A., Misra, R., Ahmod, N., Fang, M., Shah, H., and Gharbia, S. (2010). Coherent pipeline for biomarker discovery using mass spectrometry and bioinformatics. BMC Bioinformatics *11*, 437.

Andreatta, M., and Nielsen, M. (2016). Gapped sequence alignment using artificial neural networks: application to the MHC class I system. Bioinformatics *32*, 511-517.

Bassani-Sternberg, M., Barnea, E., Beer, I., Avivi, I., Katz, T., and Admon, A. (2010). Soluble plasma HLA peptidome as a potential source for cancer biomarkers. Proc Natl Acad Sci U S A *107*, 18769-18776.

Delgado, J.C., Escobar, H., Crockett, D.K., Reyes-Vargas, E., and Jensen, P.E. (2009). Identification of naturally processed ligands in the C57BL/6 mouse using large-scale mass spectrometric peptide sequencing and bioinformatics prediction. Immunogenetics *61*, 241-246.

Escobar, H., Crockett, D.K., Reyes-Vargas, E., Baena, A., Rockwood, A.L., Jensen, P.E., and Delgado, J.C. (2008). Large scale mass spectrometric profiling of peptides eluted from HLA molecules reveals N-terminal-extended peptide motifs. J Immunol *181*, 4874-4882.

Franchin, C., Pivato, M., Rattazzi, M., Arrigoni, G., and Millioni, R. (2014). OFFGEL fractionation of peptides: where really is your sample? J Chromatogr A *1355*, 278-283.

Hassing, H.C., Surendran, R.P., Derudas, B., Verrijken, A., Francque, S.M., Mooij, H.L., Bernelot Moens, S.J., Hart, L.M., Nijpels, G., Dekker, J.M., et al. (2014). SULF2 strongly prediposes to fasting and postprandial triglycerides in patients with obesity and type 2 diabetes mellitus. Obesity *22*, 1309-1316.

Hwang, J.Y., Lee, E.J., Jin Go, M., Sung, Y.A., Lee, H.J., Heon Kwak, S., Jang, H.C., Soo Park, K., Lee, H.J., Byul Jang, H., et al. (2012). Genome-wide association study identifies GYS2 as a novel genetic factor for polycystic ovary syndrome through obesity-related condition. Journal of human genetics *57*, 660-664.

Ivanova, E.A., Bechtold, D.A., Dupre, S.M., Brennand, J., Barrett, P., Luckman, S.M., and Loudon, A.S. (2008). Altered metabolism in the melatonin-related receptor (GPR50) knockout mouse. American journal of physiology. Endocrinology and metabolism *294*, E176-182.

Kall, L., Storey, J.D., MacCoss, M.J., and Noble, W.S. (2008). Posterior error probabilities and false discovery rates: two sides of the same coin. J Proteome Res *7*, 40-44.

Kim, K.E., Cho, Y.S., Baek, K.S., Li, L., Baek, K.H., Kim, J.H., Kim, H.S., and Sheen, Y.H. (2016). Lipopolysaccharide-binding protein plasma levels as a biomarker of obesity-related insulin resistance in adolescents. Korean journal of pediatrics *59*, 231-238.

Kowalewski, D.J., and Stevanovic, S. (2013). Biochemical large-scale identification of MHC class I ligands. Methods Mol Biol *960*, 145-157.

Kumar, G., Gotesman, M., and El-Matbouli, M. (2015). Interaction of Tetracapsuloides bryosalmonae, the causative agent of proliferative kidney disease, with host proteins in the kidney of Salmo trutta. Parasitol Res *114*, 1721-1727.

Lopez, I.P., Milagro, F.I., Marti, A., Moreno-Aliaga, M.J., Martinez, J.A., and De Miguel, C. (2004). Gene expression changes in rat white adipose tissue after a high-fat diet determined by differential display. Biochemical and biophysical research communications *318*, 234-239.

Moreno-Navarrete, J.M., Ortega, F., Serino, M., Luche, E., Waget, A., Pardo, G., Salvador, J., Ricart, W., Fruhbeck, G., Burcelin, R., et al. (2012). Circulating lipopolysaccharide-binding protein (LBP) as a marker of obesity-related insulin resistance. International journal of obesity *36*, 1442-1449.

Murphy, J.P., Konda, P., Kowalewski, D.J., Schuster, H., Clements, D., Kim, Y., Cohen, A.M., Sharif, T., Nielsen, M., Stevanovic, S., et al. (2017). MHC-I Ligand Discovery Using Targeted Database Searches of Mass Spectrometry Data: Implications for T-Cell Immunotherapies. J Proteome Res *16*, 1806-1816.

Ni, X., Tan, Z., Ding, C., Zhang, C., Song, L., Yang, S., Liu, M., Jia, R., Zhao, C., Song, L., et al. (2019). A region-resolved mucosa proteome of the human stomach. Nat Commun *10*, 39.

Parray, H.A., and Yun, J.W. (2015). Proteomic Identification of Target Proteins of Thiodigalactoside in White Adipose Tissue from Diet-Induced Obese Rats. International journal of molecular sciences *16*, 14441-14463.

Purcell, A.W. (2004). Isolation and characterization of naturally processed MHC-bound peptides from the surface of antigen-presenting cells. Methods Mol Biol *251*, 291-306.

Qin, S., Song, G., and Yu, Y. (2014). Phospholipid transfer protein in diabetes, metabolic syndrome and obesity. Cardiovascular & hematological disorders drug targets *14*, 149-153.

Taleux, N., Guigas, B., Dubouchaud, H., Moreno, M., Weitzel, J.M., Goglia, F., Favier, R., and Leverve, X.M. (2009). High expression of thyroid hormone receptors and mitochondrial glycerol-3-phosphate dehydrogenase in the liver is linked to enhanced fatty acid oxidation in Lou/C, a rat strain resistant to obesity. The Journal of biological chemistry *284*, 4308-4316.

Tzotzas, T., Desrumaux, C., and Lagrost, L. (2009). Plasma phospholipid transfer protein (PLTP): review of an emerging cardiometabolic risk factor. Obesity reviews : an official journal of the International Association for the Study of Obesity *10*, 403-411.

Zheng, Y., Qu, H., Xiong, X., Wang, Y., Liu, X., Zhang, L., Liao, X., Liao, Q., Sun, Z., Ouyang, Q., et al. (2019). Deficiency of Mitochondrial Glycerol 3-Phosphate Dehydrogenase Contributes to Hepatic Steatosis. Hepatology *70*, 84-97.